Effect of friction on Finite Element contact and wear predictions of metal-on-plastic hip replacements

Lorenza Mattei[1*], Francesca Di Puccio[1]

[1]Department of Civil and Industrial Engineering, Largo Lucio Lazzarino 2, Pisa, 56126, IT

Abstract

Finite Element wear predictive modelling is a powerful tool that can replace or support costly and time-consuming wear tests. Despite the lively research in this field, particularly in applications to hip replacements, some issues are still open, such as the role of friction in numerical simulations. Indeed, in most wear models, frictionless contact conditions are assumed and wear routines are independent from *f*. However, the effect of friction on contact and wear modelling of metal-on-plastic hip replacements has never been fully explored in the literature.

In this study we analyse how the friction coefficient affects both the contact features (nominal contact point trajectory, components of the contact force and contact pressure) and the wear parameters, (wear volume and linear wear distribution). A case study of a 32 mm implant was simulated under two different loading and kinematic conditions, considering both vertical and 3D load, and varying the friction coefficient *f* within the range 0-0.3, for a given *k* value. Results show that a frictional contact has longer and wider trajectories of the nominal contact point, but slightly lower normal force and contact pressure values, with respect to a frictionless solution. Consequently, contact pressure maps are shifted with respect to the frictionless case but values remain almost the same changing *f.* The wear volume slightly decreases with *f* whilst wear maps are very sensitive to it. Results suggest that so that for $f \leq 0.1$ the frictionless hypothesis can be adopted achieving accurate results with the advantage of reduced computational costs.

Keywords: frictional contact, FE wear modelling, wear map, hip prosthesis, Metal-on-plastic

1 Introduction

Numerical wear models are a powerful tool to predict long-term wear in many mechanical and biomechanical applications [1,2]. They can replace or support experimental investigations allowing sensitivity analyses to design parameters at low cost and with shortened times. In the last two decades, the research in advanced wear modelling of hip replacements (HRs) has been very lively, as demonstrated by the high number of published papers, e.g. [3–5] just to mention but a few. Many important aspects affecting the wear process have been pointed out and included in wear models, particularly for the most clinically used metal-on-plastic (MoP) implants. However, some modelling issues still require further investigations as the cross shearing phenomenon of UHMWPE [3,6,7] and the creep effect at the early running-in phase [8,9]. Additionally, more patient-specific daily activities, in addition to walking, should be simulated to achieve realistic wear predictions [10,11]. Mostly important, model validation should be considered [12,13].

On the tribological side, an aspect that deserves further attention is the effect of friction in wear models, that most frequently are based on frictionless contact hypotheses, which can appear as a contradiction.

* Corresponding author
Tel. Number: (+39) 050 2228014
Email: Lorenza.mattei@unipi.it

Indeed, friction and wear are strictly correlated and dependent on the tribological scenario of the considered coupling, i.e. macro and micro geometry, loads and kinematics, lubricant properties, etc. During a single load cycle (e.g. walking cycle), and even more during the service life of an implant, the lubrication regime can vary affecting both friction and wear [14]. However, such complicated time-varying interplay is generally simplified in wear models: dry contact conditions are assumed and the wear behaviour is considered independent from friction so that a non-null constant wear coefficient k (eventually varying on the contact surface as a function of the cross-shear ratio) is typically combined with a frictionless contact condition. Despite being not physically reasonable, these assumptions are only an apparent inconsistency and are accepted in numerical simulations to simplify the analyses and reduce the computational costs. Indeed, friction and lubrication regime affect the wear model through the coefficient k that is estimated from experimental tests. While in pin-on-disc cases, k can be easily obtained from the ratio of worn volume and the product of the normal load times the sliding distance, for hip replacements, a model is required to calculate k by comparing numerical and experimental wear volumes, the latter affected by the real lubricated contact conditions. Usually k is estimated as an average value after a rather high number of cycles.

Only a couple of studies simulate mixed lubricated contact conditions in MoP HRs [11,15], but they do not discuss the frictional effects. On the other hand, only five [16–21] out of 22 studies considered by the recent review [4] modelled frictional contact conditions assuming a constant friction coefficient f within the range 0.04-0.083 or f dependent on the contact pressure [3].

The effect of friction on contact and wear parameters has never been fully explored in the literature. Only two studies [16,22] describes the effect of the friction very marginally, only on wear volume, and even reporting opposite results. In [16] a volumetric wear decrease of 2% is predicted when f increases from 0.01 to 0.09, whilst [22] reported an increase of 12% of the volumetric wear for f=0.3, compared to the frictionless case.

The objective of this study was to investigate, through a sensitivity analysis, how a frictional contact hypothesis can affect both contact and wear features of a hip replacements, made of a metallic head and a plastic cup. As far as the contact parameters is concerned, three different aspects were explored, i.e. the effect of friction on: i) the trajectory of the nominal contact point, ii) the magnitude of the normal contact force and iii) contact pressure distribution. Additionally, the effect of frictional contact on wear results, i.e. worn volume and linear wear/wear depth were investigated. The representing of wear depth over the contact surfaces produced wear maps, that are rarely considered though fundamental for wear model validation, based on the comparison of numerical and experimental wear distributions. Several FE wear models of an MoP implant were developed assuming both frictionless and frictional contact conditions. The friction coefficient f was considered fixed throughout the wear process (i.e. in each simulation) with values ranging from 0 up to 0.3 while k was kept constant in all models being obtained from experimental tests. All simulations were run for two different sets of loading and kinematic conditions: standard ISO 14242-1 Boundary Conditions (BCs), and revised ISO conditions, so to have fixed and mobile load direction with respect to the cup. That allows a wider comprehension of the effect f on the trajectory of the contact point. Additionally, the reliability of the frictionless hypothesis is investigated as already done in [23] by these authors for pin-on-plate test simulations. Such hypothesis is useful to reduce the computational cost of HR wear models, which is one of their main limitations.

2 Methods

Case study

The developed FE models are based on the case study described in [16], with numerical and experimental investigations on a 32 mm MoP HRs with 0.46 mm diametrical clearance. Such study was selected as it describes clearly all simulated data and also reports experimental results for model validation, rarely found in the literature.

FE wear models

FE models were developed in Ansys Workbench® and some results were processed in Matlab®.

2.1.1 Geometry and materials

The geometry consists in a ball-in-socket joint as shown in Fig. 1. The head is a sphere of diameter 36 mm whilst the cup a hemispherical liner with the internal diameter of 32.46 mm and the thickenss of 15 mm. As it shown in Fig. 1(a), all the surafces were divided in sectors to help the meshing procedure and the definition of the BCs.

The cup in UHMWPE was modelled as a linear elastic material, with Young's modulus equal to 500 MPa and the poisson ratio 0.4. A more advance material model for the UHMWPE, implementing a strain hardening behaviour was adopted in [3,16,24] but not considered in this study to reduce the complexity of the model and thus to limit the computational costs of the planned sensitivity analysis. Furthermore, results are expected to be unsensitive to the material model since the friction contact condition does not affect material models adopted in [3,16,24].

Since the head is in metal and thus, much harder and stiffer than the cup, we assumed its wear neglegible and modelled it as a rigid body. That allowed to greatly reduce the computational time.

2.1.2 Mesh

The cup was meshed with hexahedral elements of second order, i.e. SOLID186 (Fig. 1(b)). The contact surfaces were meshed with CONTA174 and TARGE170 elements (see contact details in Sec. 3.2.3) (Fig. 1(c, d)). In particular, the cup mesh was obtained combining edge sizing method and multizone sweep method. The face sizing method was used for the head meshing. Correspondent elements were created for head and cup contact surfaces, with null rotations (Fig. 1(c, d)).

Element edge size was of about 1.25 mm close to the contact region up to 2 mm on the external cup surface. The mesh size was selected on the basis of a sensitivity analysis, to guarantee a percentage variation of the maximum contact pressure (in unworn conditions) of about 0.5% when reducing the element size of 36% (i.e. element edge size of 0.8 mm).

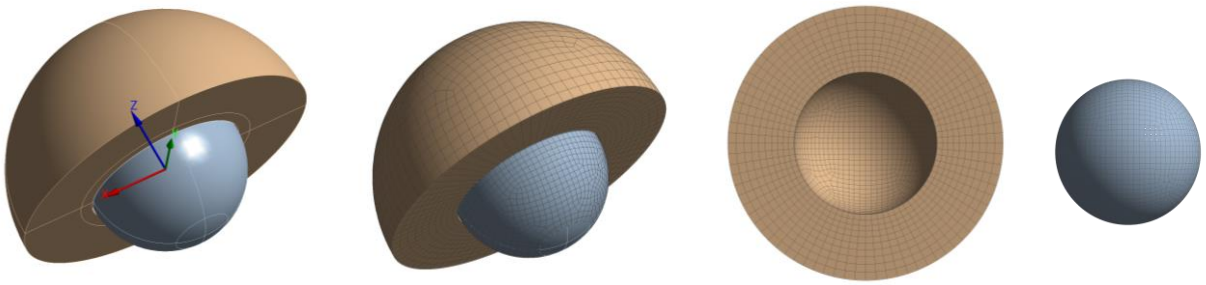

(a) (b) (c) (d)

Fig. 1 (a) Geometry of FE models of 32 mm MoP HR. (b) Mesh of models and mesh detail of the contact surfaces of cup (c) and head (d).

2.1.3 Contact conditions

The contact between the internal cup surface and head surface was defined as asymmetric in the *behavior* settings, since only the cup undergoes wear. Augmented Lagrange formulation and nodal-normal to target detection method were chosen, with the cup and head as contact and target body, respectively. The contact was simulated both as frictionless and frictional, with a friction coefficient f fixed in each simulation. A sensitivity analysis was done considering seven values of f : 0, 0.05, 0.1, 0.15, 0.2, 0.25, 0.3, which cover the range of literature data (see §3.1.4).

2.1.4 *Wear modeling*

The adopted wear model was based on the Archard wear law, usually written as

$$V = k\, L_{\mathrm{N}}\, s \qquad (1)$$

where V is worn volume, k is wear coefficient, L_{N} the load normal to the contact and s, the sliding distance. In numerical wear models, the Archard law is implemented in local form, to estimate the wear rate $\dot{h}$ in each point of the contact surface P, at a given instant t, given by

$$\dot{h}(P,t) = k\, p(P,t)\, v(P,t) \qquad (2)$$

where p is the contact pressure and v the magnitude of the sliding velocity.

The Archard wear law is implemented automatically in Ansys Workbench through *TB, WEAR* APDL command defined in the contact environment. The option *ARCH* was activated to select the generalized Archard wear law that is

$$\dot{h} = \frac{k}{H}\, p^m v^n \qquad (3)$$

where H is the material hardness, and m and n the exponents of the contact pressure and sliding velocity, respectively. The parameters H, m and n were set equal the unit through the *TBDATA* command, to obtain the desired Eq.(2). Finally, the time period during which simulate wear was defined using *TBFIELD* command.

An uncalibrated k_{uc} value of 1.066 10^{-9} mm^2/N [16,41] was assumed to run simulations. A unique calibrated k_{c} was then evaluated by comparing the numerical wear volume V^{num} to the experimental one V^{exp} obtained for the same tribological conditions at 1 Mc, i.e. for RevISO BCs with f=0.04 and Test 1 of [16], respectively (V^{exp}=30 mm^3) , according to

$$k_{\mathrm{c}} = \frac{V^{\mathrm{exp}}}{V^{\mathrm{num}}/k_{\mathrm{uc}}} \qquad (4)$$

The estimated k_{c} resulted equal to 8.983 10^{-10} mm^2/N and it was used to scale results of all simulations, by varying f value.

Wear volumes were estimated for one year of walking activity, about 1 Mc (1 Mc=10^6 cycles), corresponding approximately to the running-in phase [16]. The geometry update is implemented within a gait cycle although it did cause a variation of the contact pressure. According to the literature [40,42], we assumed that the modification of the mesh caused by material removal did not affect markedly contact pressure up to 1Mc. Consequently, results at 1 Mc were obtained simply scaling results obtained for 1 gait cycle by 10^6.

2.1.5 *Kinematic and loading conditions*

As typically done in the literature, wear was estimated for walking conditions with time-varying load and 3D head-cup relative motion. Two sets of boundary conditions, denoted as ISO and RevISO, differing only for the load direction, were simulated. The BCs were defined in the fixed coordinate frame S={O_{h}, x, y, z}, with the origin at the centre of the head O_{h} and with axes x, y and z corresponding to the flexion-estension, adduction-abduction and inward-outward rotation axes, respectively. The ISO BCs were defined according to ISO 14242-1 and were characterized by a vertical and fixed load, i.e. $\mathbf{L}_z = L(\mathrm{t})[0\ 0\ 1]$. The RevISO BCs were characterized by a load with time-varying direction fixed with respect to the head, i.e. $\mathbf{L}_{xyz} = L(\mathrm{t})\ \boldsymbol{\lambda}(\mathrm{t})$, with $\boldsymbol{\lambda}$ unit vector of the loading direction, as in [16]. As schematically represented in Fig. 2(a-b), both the load and motion were applied to the head, whilst the external cup surface was built-in. In particular, the load was applied as a remote force applied to a region of the head surface, whilst the head motion was implemented through a bushing joint, with 6 DoFs, connecting the head to the ground. The same load magnitude and rotation angles curves were simulated for the ISO and the RevISO BCs, depicted in Fig. 2 (c) and (d), respectively. The head motion is defined according to the rotation sequence flexion/extension->abduction/adduction-> inward/outward rotation, i.e FEx->AAy->IOz, defined in the fix coordinate frame S.

A sensitivity analysis with respect to the sampling frequency of the loading and kinematics curves was performed providing a convergence value of 50 Hz. The loading and kinematics curves were thus sampled uniformly every 0.02 s, for a total of 50 load steps per gait cycle.

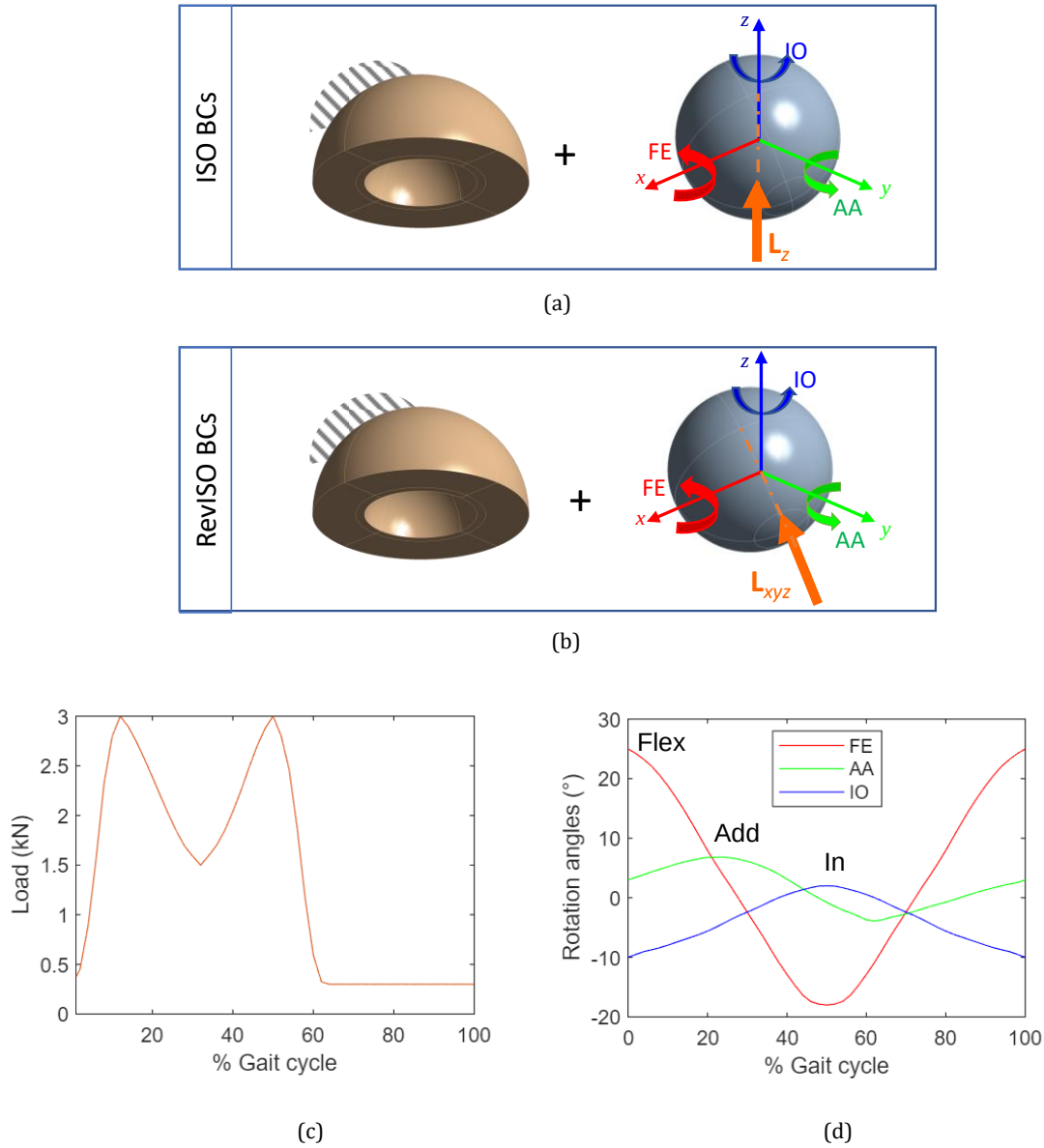

Fig. 2 3D Loading and kinematics conditions: (a) ISO BCs with vertical load, (b) RevISO BCs with mobile load, fixed with respect to the head, and (c) loads and rotation angles curves during a gait cycle.

3 Results and discussion

3.1.1 Effect of friction on contact parameters

As first effect of friction on results, the modification of the trajectory of the nominal contact point P_c during the gait cycle was examined. The latter is defined as the intersection point between the load line of action *l* and the cup/head surface, as shown in Fig. 3. As shown in Fig. 4, the presence of friction caused a wider trajectory of P_c both for ISO (Fig. 4(a)) and RevISO BCs Fig. 4(b). Under ISO BCs, for frictionless contact, P_c remained fixed on the cup since the load direction was vertical and the cup built-in. However, in case of frictional contact, P_c drew a circular trajectory on the cup, having a radius which increases with the

value of f. Under RevISO BCs, since the load direction varied during the gait cycle, P_c moved over the cup surfaces both for the frictionless and frictional contact conditions, even if, in the latter case, the trajectory travelled by P_c was longer and wider. Similarly to the previous case, the higher the f value, the longer the trajectory of P_c. These results are in good agreement with the theory. Indeed, in presence of friction, the nominal contact point P_c moves in direction opposite to the local sliding velocity, assuming a new position labelled P_c^f rotated with respect to P_c of an angle φ=atan(f), as represented in Fig. 3 where $\boldsymbol{\omega}^{rel}$ is the relative angular velocity between the head and the cup. Indeed, in presence of friction a tangential force L_T arises in the contact and, to guarantee the force equilibrium conditions, the application point of the load moves to P_c^f, thus reducing its normal component L_N=L to L cos(φ). For the moment equilibrium, a torque $\mathbf{M}_f$ is necessary to balance the torque generated by the load **L**. Further details can be found in [43].

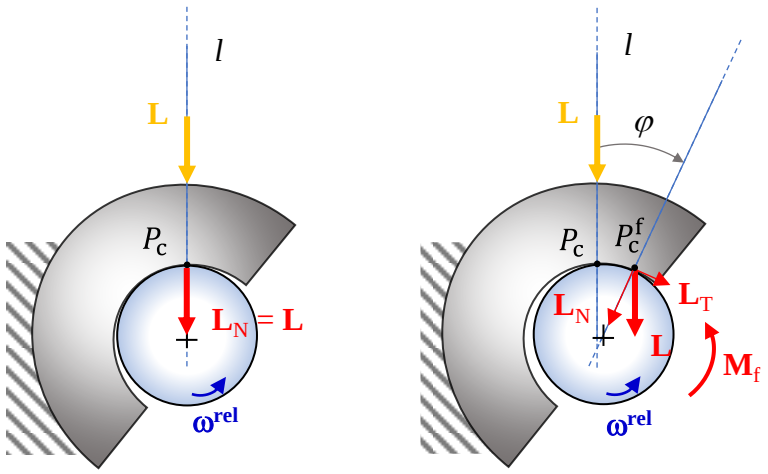

Fig. 3 Theoretical effect of friction on the nominal contact point and the normal load component.

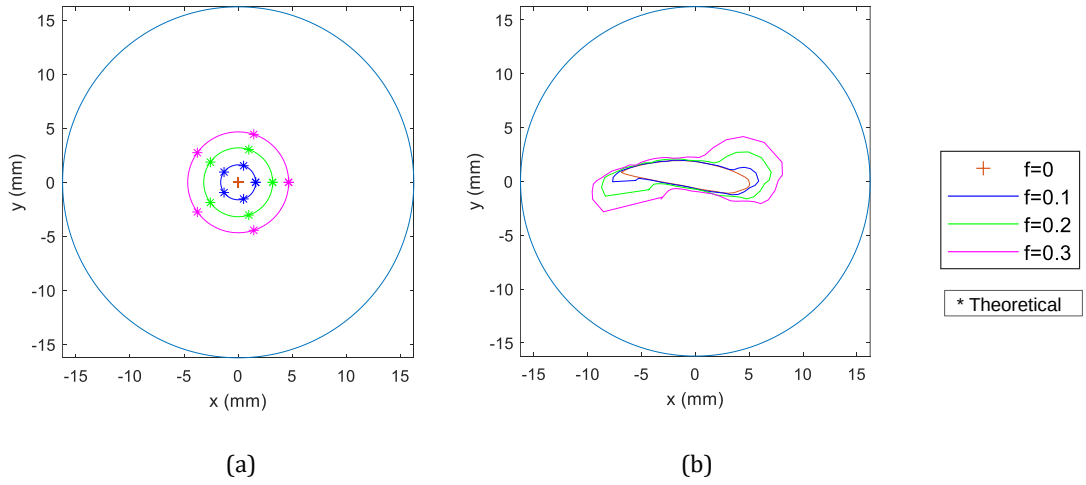

*Fig. 4 Effect of friction on the trajectory of the nominal contact point for (a) ISO and (b) RevISO BCs. Theoretical results for ISO BCs are marked with * symbol for each f/colour.*

In case of ISO BCs with fixed P_c, the wear model predicted circular trajectories centred with respect to P_c and of radius r_c sin(φ), in agreement with the theory (Fig. 4(a)). Also the normal load component predicted by our models was in agreement with the theory. Fig. 5(a) shows the effect of the friction coefficient on the normal load component, comparing the numerical and theoretical curves, that resulted overlapped. Consequently, friction caused a normal load reduction of cos(φ), that means about 7% for

f=0.3. Accordingly, also the contact pressure decreased with *f*, although non-linearly with the load. Fig. 5(b) shows the curves of the maximum contact pressure p_{max} during the gait cycle by varying *f*: the effect of the friction is not relevant since a maximum percentage variation of -3% was predicted between the frictionless and the frictional (*f*=0.3) cases.

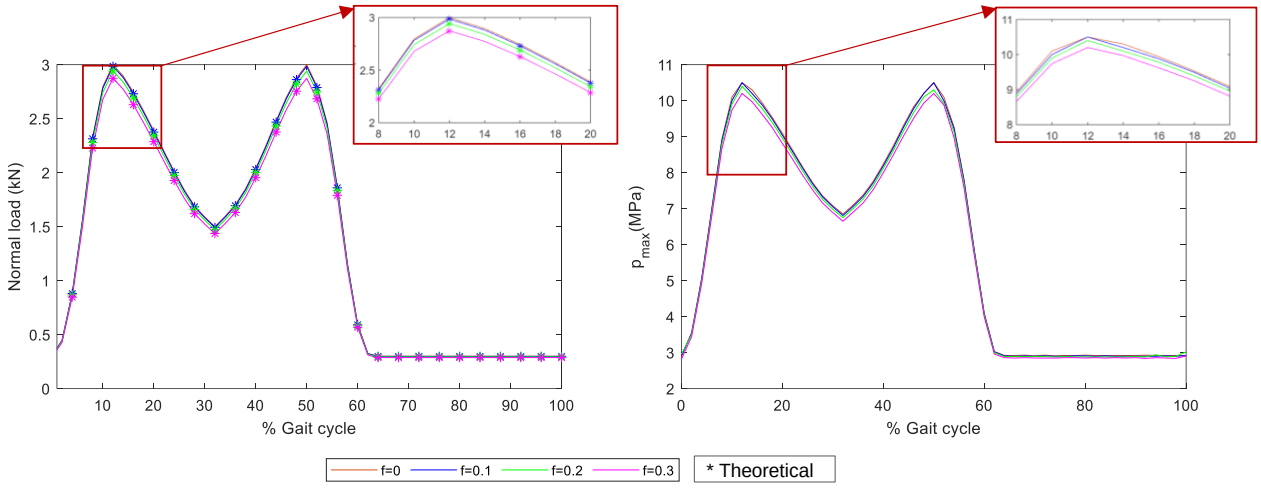

(a) (b)

*Fig. 5 Effect of friction on the magnitude of the normal load component (a) and on the maximum contact pressure (b). The curves are zoomed in correspondence of the first load peak to highlight the differences (at the top-left of the main figure). Theoretical results for the normal load component are marked with * symbol.*

The displacement of nominal contact point, combined to a reduction of normal load component, affected the contact pressure maps. The evolution of the contact pressure during the gait cycle in case of frictionless conditions is represented at the top of Fig. 6 for the RevISO BCs. Results for ISO BCs are not reported since less significant and in agreement with those of RevISO BCs. The pressure map was always symmetric with respect to the loading direction, i.e. the P_c, and thus moved on the cup surface during walking. The maximum contact pressure located at P_c and contact area increased with the load, reaching the maximum value at the two load peaks of 10.5 MPa and 574 mm^2, respectively. In case of frictional contact, the pressure maps were almost the same of the frictionless case, although located in a different position, i.e. centered at P_c^f, as shown at the bottom of Fig. 6 for the case *f*=0.3. Nevertheless, the contact pressure distribution always remained circular and symmetric with respect to P_c^f.

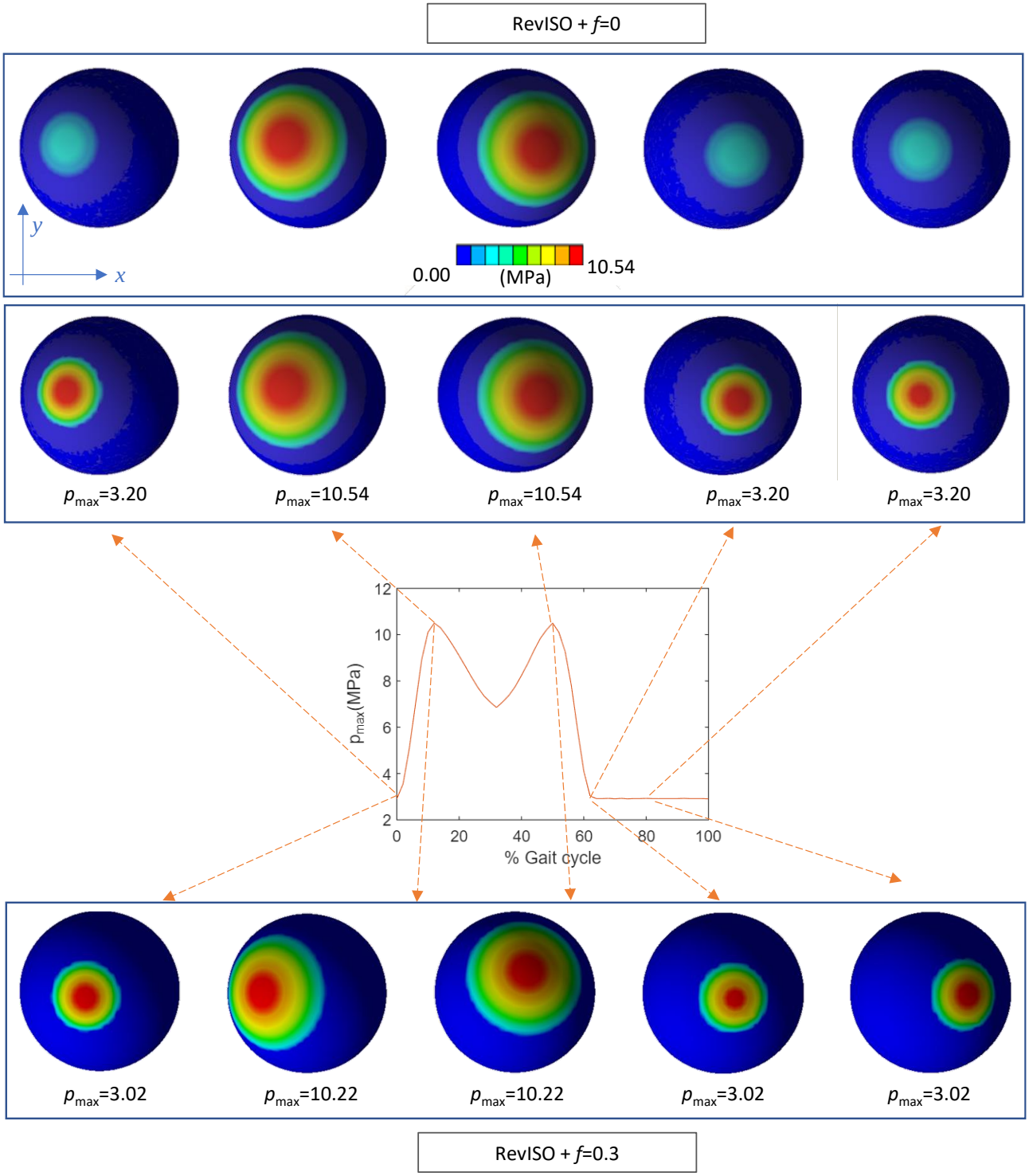

Fig. 6 Evolution of maps of the contact pressure during a gait cycle, for RevISO BCs. Comparison of the frictionless (top) and frictional cases (bottom). The pressure maps on first row are reported on the same scale whilst those ones on the second and third row are plotted each one on its own full-scale.

3.1.2 Effect of friction on wear parameters

In case of frictional contact, the reduction of the normal load is combined to an increase of the sliding distance related to the longer trajectory of the nominal contact point. Their combined effect is a reduction of the wear volume V compared to the frictionless case (given the assumption of the same value of k_c in

frictionless and frictional cases) from 28.8 to 26.9 mm^3 and from 30.08 to 28.23 mm^3 for the ISO and the RevISO BCs, respectively. As depicted in Fig. 7, similar results were obtained for the ISO and RevISO BCs: the percentage variation of V with f was non linear, with a maximum value of about -6.5% for f=0.3. The effect of the friction on wear volume is in good agreement with the literature: [16] reported a -2% change of the wear volume for f=0.09, compared to the frictionless case, versus -1% of the present study.

The wider trajectory of P_c^f in comparison with P_c, explains the wider worn area in the frictional case. Consequently, having a lower wear volume and a wider worn area, the linear wear for frictional cases resulted much lower (0.123 vs 0.096 mm for ISO BCs, and 0.115 vs 0.089 mm for RevISO BCs). The percentage variation of the maximum wear depth h_{max} with f value is plotted in Fig. 7: the trend was non-linear as for V, but the variation was higher, up to -21.4% for f=0.3. Again, almost overlapped curves of percentage variation of h_{max} were obtained for ISO and RevISO BCs.

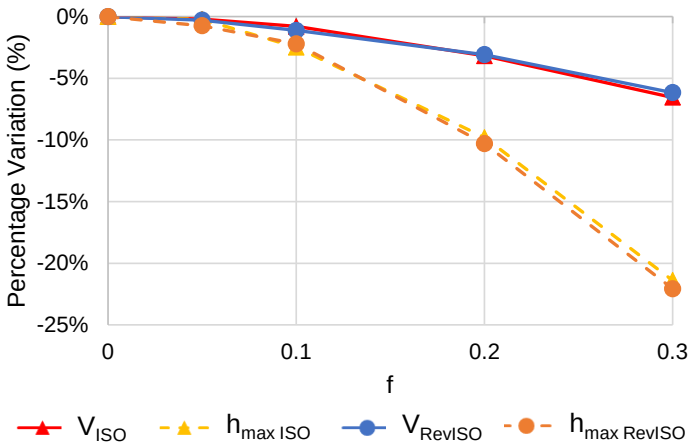

Fig. 7 Effect of the friction on wear volume V and maximum wear depth h_{max}, at the first load peak.

The effect of friction on wear maps is presented in Fig. 8 and Fig. 9 for the ISO and RevISO BCs, respectively. The wear maps obtained for f values of 0, 0.1, 0.2 and 0.3 are compared, represented both on full scale (central column) and on the same scale (column on the right). To facilitate the maps comprehension, also the trajectories of P_c and P_c^f, are reported.

Starting from the ISO BCs case, in frictionless conditions, the map of the contact pressure was centred on the cup pole (P_c) during the whole gait cycle, thus the wear map resulted circular and symmetric with respect to the cup pole. As the friction coefficient increased from 0.1 to 0.3, P_c^f covered circles with increasing radii and, accordingly, the worn area increased as well, resulting stretched in the lateral direction (negative x axis). That can be explained considering that P_c^f occupies positions in the central-lateral region during the high-load stance phase of the gait cycle, whilst it moved to the medial region in the swing phase. The comparison of wear maps for different f values when reported on the same scale clearly showed that the higher the friction coefficient the lower h_{max}. These results were confirmed by wear predictions for the RevISO BCs (see Fig. 9). In this case, in frictionless conditions the wear map is slightly stretched in medio-lateral direction, accordingly to the shape of the P_c trajectory. The wear map is even more stretched in the same direction for high friction values, because, as for the ISO BCs, P_c^f covered the lateral-central region during the stance phase. For both sets of BCs, wear maps for f=0.05 were not reported since very similar to the frictionless results.

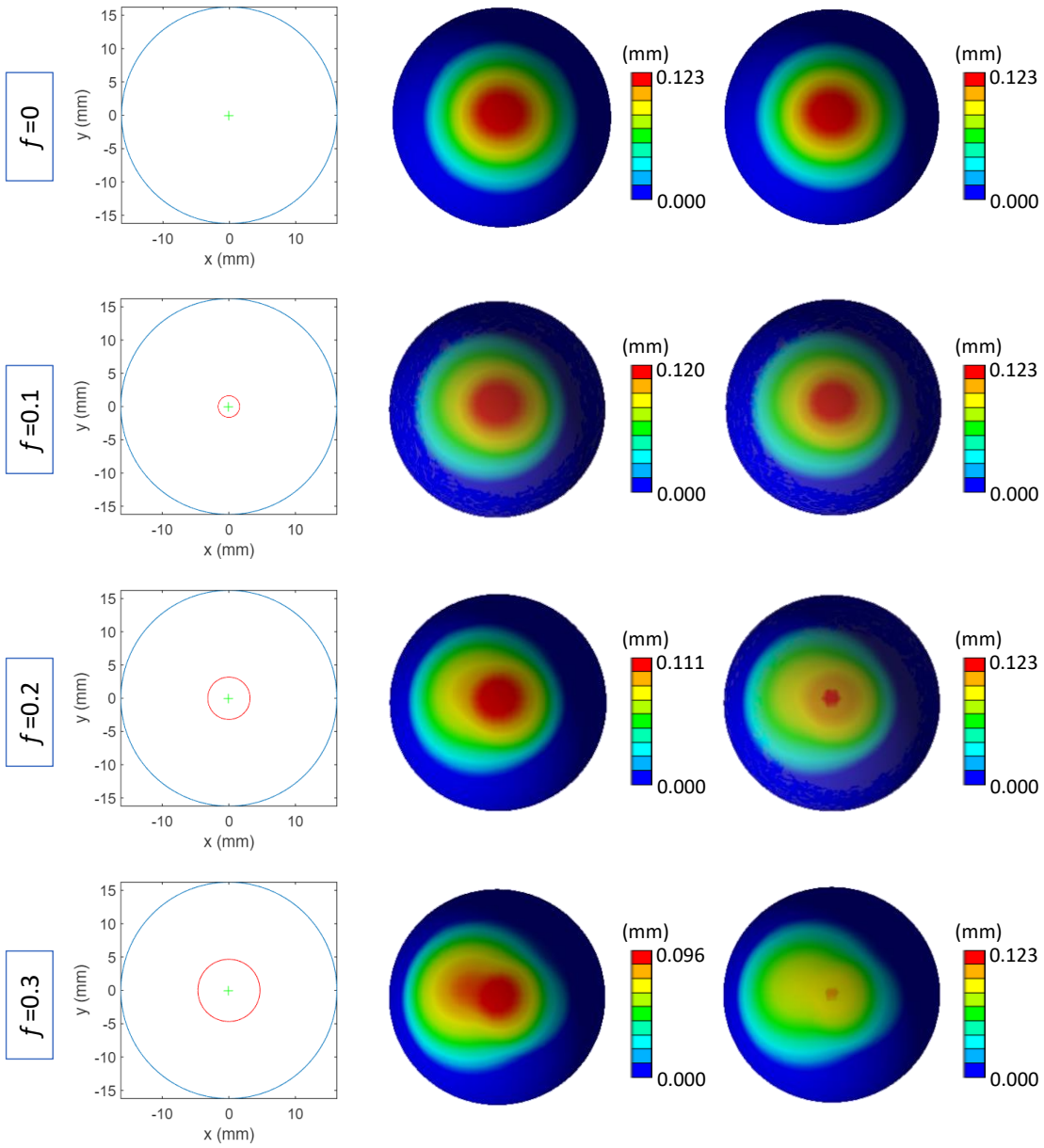

Fig. 8 Effect of the friction on wear maps for the ISO BCs. Wear maps are reported at full scale (central column) and on the same scale (right column). For a better comprehension, also the trajectories of the nominal contact point are plotted in the left column.

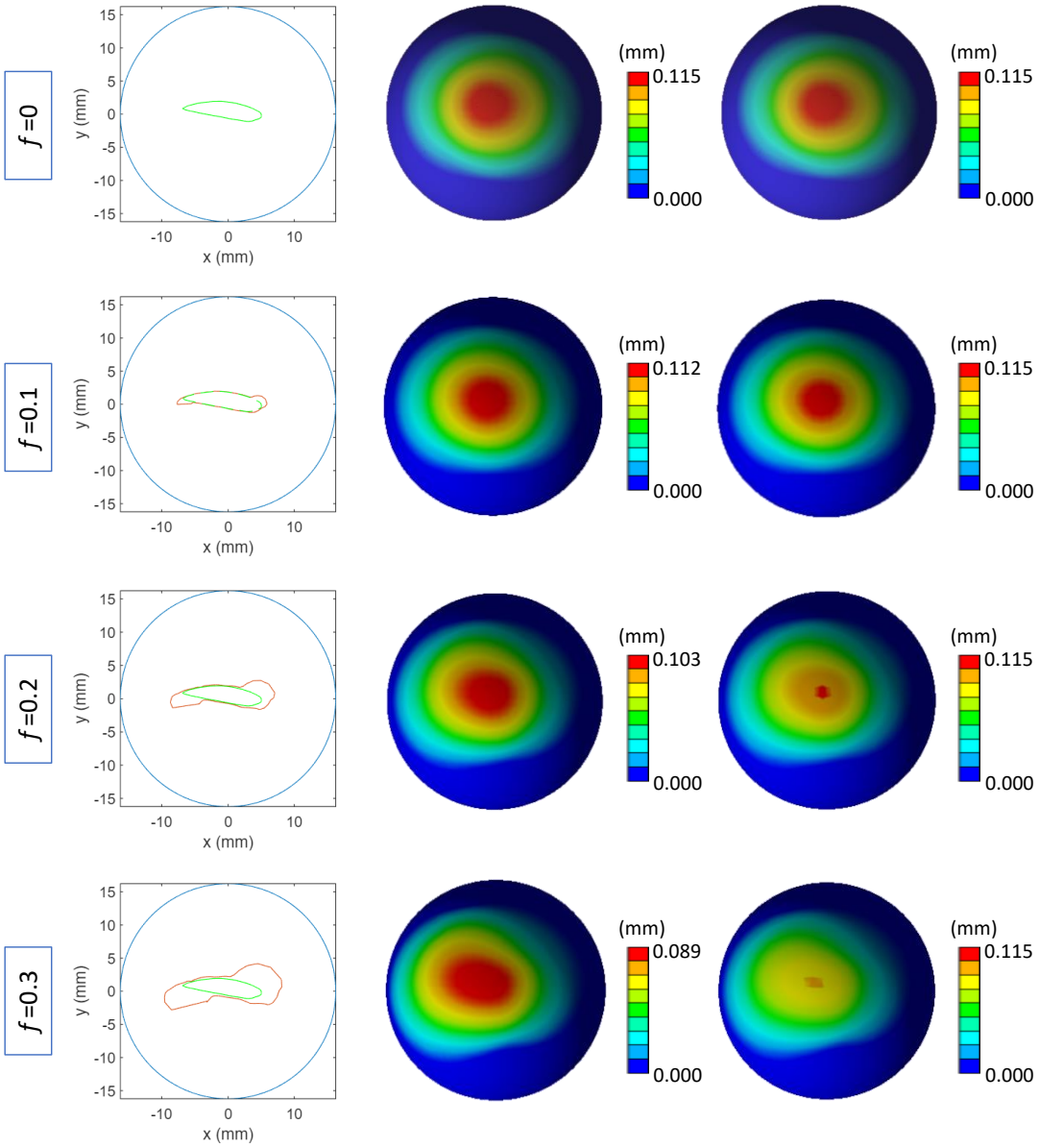

Fig. 9 Effect of the friction on wear maps for the RevISO BCs. Wear maps are reported at full scale (central column) and on the same scale (right column). For a better comprehension, also the trajectories of the nominal contact point are plotted in the left column.

3.1.3 Effect of friction on computational costs

The effect of friction on the simulation time is described by the histogram in Fig. 10. According to the literature [23], the simulation of a frictional contact caused longer computational times. For both the simulated BCs, the computational time was minimum for frictionless case and increased almost linearly with f: when passing from f=0 to f=0.3 it was more than threefold. To note that the simulation of ISO and RevISO BCs required similar computational costs, but higher in case of RevISO because of the time-varying loading direction.

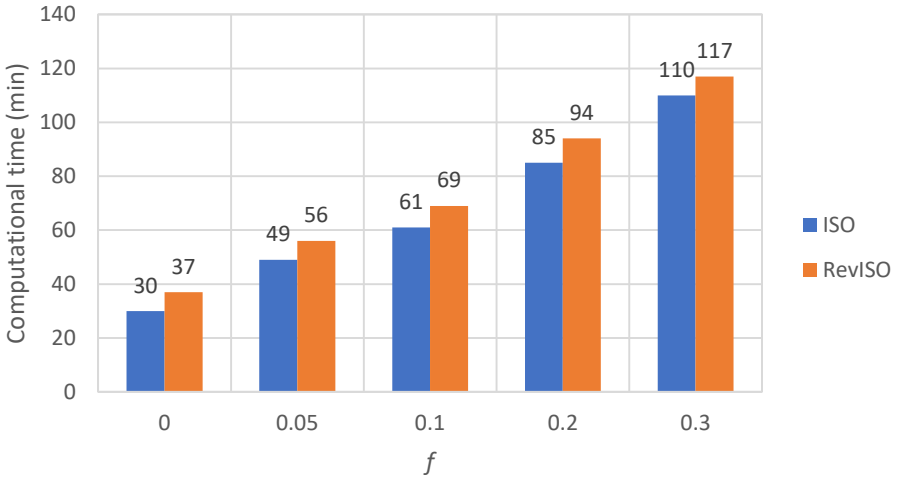

Fig. 10 Effect of the friction on the computational costs of simulations.

3.1.4 Discussion on model simplifications

The proposed models were based on some simplifying hypotheses discussed below.

a) Hypothesis on the friction coefficient

First of all, a constant friction coefficient was simulated, within the range 0-0.3 in agreement with the literature. As reviewed in [25], wear models of MoP HR typically assume a frictionless contact, i.e. f=0. More rarely, e.g. [16–21], a non-null constant value of f is considered with values in the range 0.04-0.08. Such values are in agreement with those estimated through hip joint simulator [26–28]. We note that the hypothesis of constant f is an important simplification since the friction coefficient f is markedly affected by the tribological conditions of the contact, from the load to the lubrication regime, and thus can vary locally and in time, i.e. $f(P,t)$. Only in the recent wear model on MoP HRs presented in [1], f was assumed dependent on the contact pressure, i.e. $f(p)$, with a relationship obtained from multidirectional pin-on-disc tests of metal-on-UHMWPE [29]. According to the latter, the friction coefficient was higher at lower contact pressure assuming values up to 0.3. Estimations of the friction coefficient from in-vivo measurements are described in [14,30] for ceramic-on-plastic HRs: the friction coefficient varied during the walking cycle in the range 0.01-0.125, with an average value lower than 0.05 and high values (0.125) for low loads.

Therefore, we assumed a constant f (within in each analysis) for two main considerations: firstly, the only law $f(p)$ available in the literature was estimated for pin-on-disc couplings [29], much different from HRs tribological pairs; secondly, according to *in-vivo* measurements, f was very low and mainly constant within a gait cycle with peak values for a limited interval, at the transition between the stance and the swing load phase (<15% of the cycle).

b) The role of the friction coefficient in the Archard wear law

In the Archard wear law (Eqq.(1-2)), traditionally, the friction does not appear explicitly, though it affects all terms: k, p and v. Accordingly, it can be rewritten as

$$\dot{h}(f,P,t) = k(f)\, p(f,P,t)\, v(f,P,t) \tag{5}$$

where f, as mentioned above, can vary locally and in time, i.e. $f(P,t)$.

As far as the model implementation is concerned, the dependence of p and v on f is automatically captured by simulating frictional contact conditions, whilst the law $k(f)$ should be explicitly introduced in the model. In fact, as already mentioned, in *FE* programs f and k are considered as independent input. However, in the literature, the relationship $k(f)$ has never been investigated for HRs so an experimental law of k variation during a single wear cycle is not available. Indeed, the estimation of $k(f)$ is quite hard for 3D

complex contact problems such as in hip replacements, where f varies continuously, as previously discussed, while k is estimated over a given number of wear cycles. Therefore, typically only one value of k is provided for a coupling, or, in the best scenario, two distinct values are estimated for the running-in and the steady state phases [31]. This explains why all wear models in the literature, even the most recent one [1], are based on wear coefficient constant with respect to f.

Consequently, in our study we just considered the effect of f on p and v, and used for k always the same value, estimated with the experimental wear volume, that suffices to our aim, i.e. to understand if frictional contact must be simulated to achieve accurate results or it can be avoided thus reducing extremely computational costs.

c) The role of the friction in the cross-shear based wear laws

Another fundamental aspect to be discussed is the use of the Archard wear law for the UHMWPE. The literature reports several advanced wear laws for UHMWPE surfaces in multi-directional sliding against harder counter faces, i.e. considering the cross-shearing phenomenon [25]. Such wear laws can be grouped in two parts: wear laws not explicitly dependent on friction [3,6,32–36] and wear laws based on traction forces and thus explicitly dependent on f [37–39]. The formers are based on a wear coefficient dependent on the cross-shear ratio, given by the ratio of frictional work performed in direction normal to principal molecular orientation and the total one, during a wear cycle (e.g. a gait). Since, in the wear law implementation, the friction coefficient is considered constant during the wear cycle, it is simplified and disappears in the wear coefficient function. Consequently, the effect of friction adopting such wear laws is expected to be the same of the Archard wear laws. Additionally, considering the higher computational costs of CS-based wear laws, they were not considered in the present study. These wear laws were explored by the present authors in previous works on wear modelling of MoP HRs [40,7] and are used in recent studies, such as [32]. On the other hand, the wear laws based on the traction forces, might lead to a different effect of the friction coefficient on wear predictions, with respect to the Archard wear law. The implementation of such complicated wear models goes beyond the aim of the present study, however they will be considered in future investigations.

d) The geometry changes due to creep and wear/ creep modeling

Another aspect that deserves attention regards the creep of the plastic cup that was not considered in the present study. Consequently, the only geometry modification modeled was caused by the material removal due to wear damage. Although some literature studies describe the creep to be important at the beginning of the wear process [3,16], it is not modelled in most of wear models on MoP HRs [25]. Moreover, it is expected to change only qualitatively the wear results, without modifying the overall effect of friction on wear output, since it is not affected by the contact frictional/frictionless formulation. Indeed, creep just causes a more conformal contact [3,4,16]. Simulating 1 Mc and neglecting creep allowed to reduce the computational cost of each simulation and carry out a sensitivity analysis with respect to f values, for two different sets of BCs. In future studies, the present model will be improved by simulating up to 5 Mc, i.e. 5 years of implant life, in presence of creep.

4 Conclusions

The present study investigates the effect of frictional contact conditions on contact features and wear evolution. Results pointed out that, although the effect of friction on the contact pressure is negligible, it can affect the wear volume and mostly wear maps, causing a reduction of V and h_{max} for the considered loading and kinematic conditions. Significant changes in wear predictions were observed for f values higher than 0.1 thus suggesting that, for these cases, the contact must be simulated as frictional. The modification of the wear maps with the friction coefficient is a critical point that deserves attention: the wear map is fundamental for model validation [13,42], based on the comparison of numerical and experimental wear maps. Thus, an accurate wear map prediction is essential and must be addressed including frictional

contact simulation for cases with high friction coefficient. On the other hand, frictionless conditions can be assumed when $f \leq 0.1$: accurate results are achieved with the advantage of reduced computational costs compared with the frictional cases.

The proposed models are based on some simplifying hypotheses that allowed to reduce computational costs and thus to perform a sensitivity analysis with respect to f values. However, future investigations will be devoted to improve the model considering longer implant lifetime and geometry modification caused by both wear and creep. The effect of friction will be also explored for wear laws different from the Archard one, considering cross-shearing and friction tractions.

5 References

[1] F. Di Puccio, L. Mattei, In-silico Analytical Wear Predictions: Application to Joint Prostheses, in: Wear in Advanced Engineering Applications and Materials, WORLD SCIENTIFIC (EUROPE), 2022: pp. 123–148. https://doi.org/10.1142/9781800610699_0005.

[2] L. Mattei, C. Curreli, F. Di Puccio, In-silico Finite Element Wear Predictions, in: Wear in Advanced Engineering Applications and Materials, WORLD SCIENTIFIC (EUROPE), 2022: pp. 149–172. https://doi.org/10.1142/9781800610699_0006.

[3] F. Liu, Y. He, Z. Gao, D. Jiao, Enhanced computational modelling of UHMWPE wear in total hip joint replacements: The role of frictional work and contact pressure, Wear. 482–483 (2021) 203985. https://doi.org/10.1016/j.wear.2021.203985.

[4] L. Wang, G. Isaac, R. Wilcox, A. Jones, J. Thompson, Finite element analysis of polyethylene wear in total hip replacement: A literature review, Proc Inst Mech Eng H. 233 (2019) 1067–1088. https://doi.org/10.1177/0954411919872630.

[5] L. Mattei, F. Di Puccio, B. Piccigallo, E. Ciulli, Lubrication and wear modelling of artificial hip joints: A review, Tribology International. 44 (2011) 532–549. https://doi.org/10.1016/j.triboint.2010.06.010.

[6] L. Kang, A.L. Galvin, J. Fisher, Z. Jin, Enhanced computational prediction of polyethylene wear in hip joints by incorporating cross-shear and contact pressure in additional to load and sliding distance: Effect of head diameter, Journal of Biomechanics. 42 (2009) 912–918. https://doi.org/10.1016/j.jbiomech.2009.01.005.

[7] L. Mattei, F. Di Puccio, E. Ciulli, A comparative study of wear laws for soft-on-hard hip implants using a mathematical wear model, Tribology International. 63 (2013) 66–77. https://doi.org/10.1016/j.triboint.2012.03.002.

[8] J. Zeman, M. Ranuša, M. Vrbka, J. Gallo, I. Křupka, M. Hartl, UHMWPE acetabular cup creep deformation during the run-in phase of THA's life cycle, Journal of the Mechanical Behavior of Biomedical Materials. 87 (2018) 30–39. https://doi.org/10.1016/j.jmbbm.2018.07.015.

[9] F. Liu, J. Fisher, Z. Jin, Computational modelling of polyethylene wear and creep in total hip joint replacements: Effect of the bearing clearance and diameter, Proceedings of the Institution of Mechanical Engineers, Part J: Journal of Engineering Tribology. 226 (2012) 552–563. https://doi.org/10.1177/1350650112441908.

[10] L. Mattei, M. Tomasi, A. Artoni, E. Ciulli, F. Di Puccio, Combination of musculoskeletal and wear models to investigate the effect of daily living activities on wear of hip prostheses, Proceedings of the Institution of Mechanical Engineers, Part J: Journal of Engineering Tribology. 235 (2021) 2675–2687. https://doi.org/10.1177/13506501211058239.

[11] G. Srivastava, N. Christian, C. Fred Higgs, A predictive framework of the tribological impact of physical activities on metal-on-plastic hip implants, Biotribology. 25 (2021) 100156. https://doi.org/10.1016/j.biotri.2020.100156.

[12] N. Kottan, N.H. Gowtham, B. Basu, Development and Validation of a Finite Element Model of Wear in UHMWPE Liner Using Experimental Data From Hip Simulator Studies, Journal of Biomechanical Engineering. 144 (2022) 031001. https://doi.org/10.1115/1.4052373.

[13] L. Mattei, F. Di Puccio, E. Ciulli, A. Pauschitz, Experimental investigation on wear map evolution of ceramic-on-UHMWPE hip prosthesis, Tribology International. 143 (2020) 106068. https://doi.org/10.1016/j.triboint.2019.106068.

[14] P. Damm, A. Bender, G. Duda, G. Bergmann, In vivo measured joint friction in hip implants during walking after a short rest, PLoS ONE. 12 (2017) e0174788. https://doi.org/10.1371/journal.pone.0174788.

[15] A. Ruggiero, A. Sicilia, S. Affatato, In silico total hip replacement wear testing in the framework of ISO 14242-3 accounting for mixed elasto-hydrodynamic lubrication effects, Wear. 460–461 (2020) 203420. https://doi.org/10.1016/j.wear.2020.203420.
[16] G. Matsoukas, R. Willing, I.Y. Kim, Total Hip Wear Assessment: A Comparison Between Computational and In Vitro Wear Assessment Techniques Using ISO 14242 Loading and Kinematics, Journal of Biomechanical Engineering. 131 (2009) 041011. https://doi.org/10.1115/1.3049477.
[17] J. Onişoru, L. Capitanu, A. Iarovici, Prediction of Wear of Acetabulum Inserts Due to Multiple Human Routine Activities, (2006).
[18] S. Barreto, J. Folgado, P.R. Fernandes, J. Monteiro, The Influence of the Pelvic Bone on the Computational Results of the Acetabular Component of a Total Hip Prosthesis, Journal of Biomechanical Engineering. 132 (2010) 054503. https://doi.org/10.1115/1.4001031.
[19] J.C. Fialho, P.R. Fernandes, L. Eça, J. Folgado, Computational hip joint simulator for wear and heat generation, Journal of Biomechanics. 40 (2007) 2358–2366. https://doi.org/10.1016/j.jbiomech.2006.12.005.
[20] G. Matsoukas, I.Y. Kim, Design Optimization of a Total Hip Prosthesis for Wear Reduction, Journal of Biomechanical Engineering. 131 (2009) 051003. https://doi.org/10.1115/1.3049862.
[21] S.M. Kurtz, J.A. Ochoa, C.B. Hovey, C.V. White, Simulation of initial frontside and backside wear rates in a modular acetabular component with multiple screw holes, Journal of Biomechanics. 32 (1999) 967–976. https://doi.org/10.1016/S0021-9290(99)00043-3.
[22] S.H. Teoh, W.H. Chan, R. Thampuran, An elasto-plastic finite element model for polyethylene wear in total hip arthroplasty, Journal of Biomechanics. 35 (2002) 323–330. https://doi.org/10.1016/S0021-9290(01)00215-9.
[23] L. Mattei, F. Di Puccio, Frictionless vs. frictional contact in numerical wear predictions of conformal and non-conformal sliding couplings (Accepted for publication), Tribology Letters. (2022).
[24] F. Liu, A. Galvin, Z. Jin, J. Fisher, A New Formulation for the Prediction of Polyethylene Wear in Artificial Hip Joints, Proc Inst Mech Eng H. 225 (2011) 16–24. https://doi.org/10.1243/09544119JEIM819.
[25] L. Wang, G. Isaac, R. Wilcox, A. Jones, J. Thompson, Finite element analysis of polyethylene wear in total hip replacement: A literature review, Proc Inst Mech Eng H. 233 (2019) 1067–1088. https://doi.org/10.1177/0954411919872630.
[26] A. Wang, A. Essner, R. Klein, Effect of contact stress on friction and wear of ultra-high molecular weight polyethylene in total hip replacement, Proc Inst Mech Eng H. 215 (2001) 133–139. https://doi.org/10.1243/0954411011533698.
[27] V. Saikko, Friction measurement in a hip wear simulator, Proc Inst Mech Eng H. 230 (2016) 366–372. https://doi.org/10.1177/0954411915610602.
[28] H. Haider, J.N. Weisenburger, K.L. Garvin, Simultaneous measurement of friction and wear in hip simulators, Proc Inst Mech Eng H. 230 (2016) 373–388. https://doi.org/10.1177/0954411916644476.
[29] V. Saikko, Effect of contact pressure on wear and friction of ultra-high molecular weight polyethylene in multidirectional sliding, Proc Inst Mech Eng H. 220 (2006) 723–731. https://doi.org/10.1243/09544119JEIM146.
[30] P. Damm, J. Dymke, R. Ackermann, A. Bender, F. Graichen, A. Halder, A. Beier, G. Bergmann, Friction in Total Hip Joint Prosthesis Measured In Vivo during Walking, PLoS ONE. 8 (2013) e78373. https://doi.org/10.1371/journal.pone.0078373.
[31] L. Mattei, F. Di Puccio, Influence of the wear partition factor on wear evolution modelling of sliding surfaces, International Journal of Mechanical Sciences. 99 (2015) 72–88. https://doi.org/10.1016/j.ijmecsci.2015.03.022.
[32] A. Abdelgaied, J. Fisher, L.M. Jennings, A comprehensive combined experimental and computational framework for pre-clinical wear simulation of total knee replacements, Journal of the Mechanical Behavior of Biomedical Materials. 78 (2018) 282–291. https://doi.org/10.1016/j.jmbbm.2017.11.022.
[33] L. Kang, A.L. Galvin, T.D. Brown, J. Fisher, Z.-M. Jin, Wear simulation of ultra-high molecular weight polyethylene hip implants by incorporating the effects of cross-shear and contact pressure, Proc Inst Mech Eng H. 222 (2008) 1049–1064. https://doi.org/10.1243/09544119JEIM431.
[34] L. Kang, A.L. Galvin, T.D. Brown, Z. Jin, J. Fisher, Quantification of the effect of cross-shear on the wear of conventional and highly cross-linked UHMWPE, Journal of Biomechanics. 41 (2008) 340–346. https://doi.org/10.1016/j.jbiomech.2007.09.005.

[35] M.A. Strickland, M.R. Dressler, M. Taylor, Predicting implant UHMWPE wear in-silico: A robust, adaptable computational–numerical framework for future theoretical models, Wear. 274–275 (2012) 100–108. https://doi.org/10.1016/j.wear.2011.08.020.
[36] M.R. Dressler, M.A. Strickland, M. Taylor, T.D. Render, C.N. Ernsberger, Predicting wear of UHMWPE: Decreasing wear rate following a change in direction, Wear. 271 (2011) 2879–2883. https://doi.org/10.1016/j.wear.2011.06.006.
[37] S.P. Mell, M.A. Wimmer, H.J. Lundberg, Sensitivity of total knee replacement wear to variability in motion and load input: A parametric finite element analysis study, Journal of Orthopaedic Research. 38 (2020) 1538–1549. https://doi.org/10.1002/jor.24755.
[38] S.T. O'Brien, E.R. Bohm, M.J. Petrak, U.P. Wyss, J.-M. Brandt, An energy dissipation and cross shear time dependent computational wear model for the analysis of polyethylene wear in total knee replacements, Journal of Biomechanics. 47 (2014) 1127–1133. https://doi.org/10.1016/j.jbiomech.2013.12.017.
[39] T. Schwenke, M.A. Wimmer, Cross-shear in metal-on-polyethylene articulation of orthopaedic implants and its relationship to wear, Wear. 301 (2013) 168–174. https://doi.org/10.1016/j.wear.2013.01.069.
[40] L. Mattei, F. Di Puccio, T.J. Joyce, E. Ciulli, Numerical and experimental investigations for the evaluation of the wear coefficient of reverse total shoulder prostheses, Journal of the Mechanical Behavior of Biomedical Materials. 55 (2016) 53–66. https://doi.org/10.1016/j.jmbbm.2015.10.007.
[41] T.A. Maxian, T.D. Brown, D.R. Pedersen, J.J. Callaghan, Adaptiive finite element modeling of long-term polyethylene wear in total hip arthroplasty, Journal of Orthopaedic Research. 14 (1996) 668–675.
[42] F. Di Puccio, L. Mattei, A novel approach to the estimation and application of the wear coefficient of metal-on-metal hip implants, Tribology International. 83 (2015) 69–76. https://doi.org/10.1016/j.triboint.2014.10.023.
[43] L. Mattei, F. Di Puccio, Wear Simulation of Metal-on-Metal Hip Replacements With Frictional Contact, Journal of Tribology. 135 (2013) 021402. https://doi.org/10.1115/1.4023207.